Electronic Band Structure, Effective Masses, Optical Absorption and Dielectric Function of Rutile Titanium Dioxide

C. Persson[1], J. S. de Almeida[2], N. Souza Dantas[3,4,5], R. Ahuja[2], E. F. da Silva Jr.[6], I. Pepe[3] and A. Ferreira da Silva[3]

[1] *Applied Materials Physics, Department of Materials Science and Engineering, Royal Institute of Tecnology, SE–100 44 Stockholm, Sweden*

[2] *Condensed Matter Theory Group, Department of Physics, Uppsala University, SE–751 21 Uppsala, Sweden*

[3] *Instituto de Fisica, Universidade Federal da Bahia, Campus Ondina, 40210-340 Salvador-BA, Brazil*

[4] *Departamento de Ciências Exatas, Área de Informática, Universidade Estadual de Feira de Santana, 44031 460 Feira de Santana,Bahia, Brazil*

[5] *Instituto Nacional de Pesquisas Espaciais-INPE/LAS, 12210- 970 S. J. dos Campos, SP, Brazil*

[6] *Departamento de Fisica, Universidade Federal de Pernambuco, Cidade Universitária, 50670–901, Recife-PE, Brazil*

Abstract: The electronic band structure, effective masses and optical properties of rutile phase of titanium dioxide TiO_2 are calculated employing a fully relativistic, full-potential linearized augmented plane-wave (FPLAPW) method within the local density approximation (LDA). The LDA is improved by an on-site Coulomb self-interaction correction (SIC) potential as represented in the LDA+U^{SIC} approach. The calculated fundamental band-gap energy E_g agrees very well with photoacoustic spectroscopy measurements. The effective masses are obtained directly from the curvature of the electronic band structure, taken into account the spin-orbit interaction which has a very strong affect on the band curvatures of the valence-band maximum. We also present the anisotropic dielectric function $\varepsilon(\omega) = \varepsilon_1(\omega) + i\varepsilon_2(\omega)$, as well as the static $\varepsilon_1(0)$ and high-frequency $\varepsilon_1(0<<\omega<<E_g/\hbar)$ dielectric constants. The calculated values are in good agreement with the experimental results.

INTRODUCTION

TiO_2 is a promising oxide for fabricating thin dielectrics in for instance dynamic random access memory (DRAM) storage capacitors [1], and as gate dielectrics of metal-oxide-semiconductor field effect transistor (MOSFET) [2]. Transition-metal oxidies and TiO_2 is also one of the major supports widely used in heterogeneous catalysis [3].

Many electronic and optical properties of TiO_2 are determined by their electronic band-edge structure, i.e., the energy position, the band curvature, and the band symmetry of the conduction-band minimum and the valence-band maximum. The effective electron and hole masses (i.e., the curvatures of the band edges) are used in various measurement analysis and transport simulations. Today, most theoretical studies of the electronic structures of condensed matters rely on the local density approximation (LDA) which generally yields overall accurate band structures for most materials. However, for semiconductors LDA suffers from a major problem, namely that the band-gap energy E_g is strongly underestimated. Normally, this underestimate is about 50%, but for several important semiconductors like Ge, InN and InAs the LDA band gap is even zero [4]. This LDA failure will has also an affect on the calculated effective masses [4]. Thus, in order to study details in the electronic band-edge structure like the effective electron and hole masses, one needs to apply a proper correction to the LDA potential.

In this paper, we study the electronic band-edge structure of the stable high temperature phase rutile of TiO_2 by means of a fully relativistic, full-potential linearized augmented plane-wave (FPLAPW) method [5,6] using the LDA+U^{SIC} potential [7], i.e., the LDA potential together with a modeled on-site self-interaction correction (SIC) potential. This correction potential is important to include for accurately calculating and predicting electronic and optical properties near the electronic band edges of semiconductors. We present the LDA+U^{SIC} electronic structure $E_j(\mathbf{k})$ of the conduction-band minimum and the valence-band maximum. It has been shown [4] that this LDA+U^{SIC} approach yields very good electronic and optical properties of *sp*-hybridized group-IVs, III-Vs, and II-VIs semiconductors. We show here that the potential yield an accurate band-edge structure also for rutile TiO_2. Using the LDA+U^{SIC} potential, the effective electron and hole masses as well as the optical properties in terms of the dielectric function are presented. Both the effective electron m_c and hole m_v masses show strong anisotropic electronic band edges. The effective masses are screened by the electric field from vibrations of the longitudinal optical (LO) phonons, and we therefore calculate also the corresponding polaron masses. The optical properties are calculated within the linear response theory for $|\mathbf{k}'-\mathbf{k}| = 0$. We present the anisotropic dielectric function $\varepsilon(\omega) = \varepsilon_1(\omega) + i\varepsilon_2(\omega)$, as well as the static $\varepsilon_1(0)$ and high-frequency $\varepsilon_1(0<<\omega<<E_g/\hbar)$ dielectric constants.

COMPUTATIONAL METHOD

The calculation of the electronic structure is based on the fully relativistic FPLAPW method [5], using about 850 plane waves, and the modified tetrahedron **k**-space integration with a Γ-centered mesh of 30 **k**-points together. It is a well known fact, that the LDA

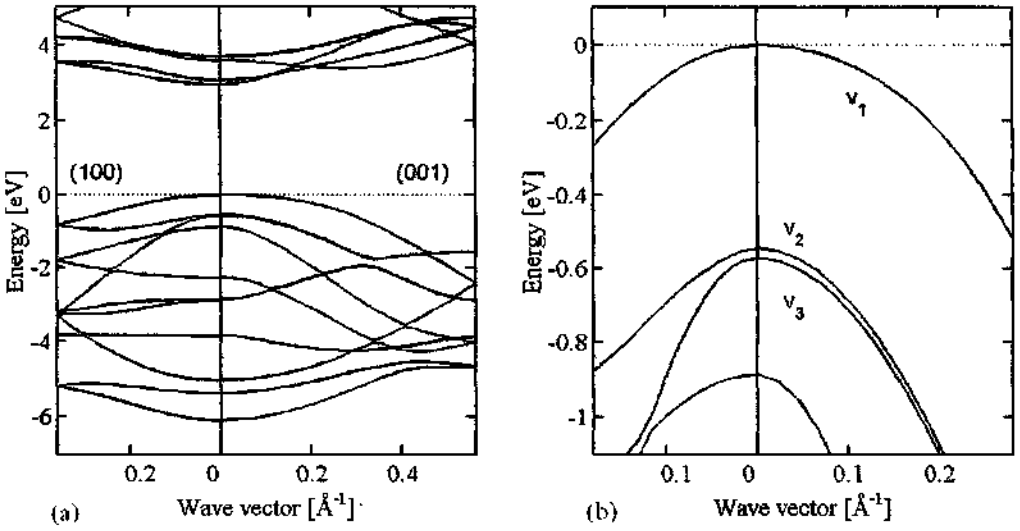

Figure 1. (a) Electronic band structure of rutile TiO_2. (b) Close-up near the Γ-point valence-band maximum.

The effective mass tensor $m(\mathbf{k})$ is defined as $1/m(\mathbf{k})_{ij} = \pm\, \partial^2 E_j(\mathbf{k})/\hbar^2 \partial k_i \partial k_j$ where + (–) stands for electrons (holes). Here, the effective masses are determined in three **k**-space directions directly from the FPLAPW electronic energies. Due to the ionic character of the titanium and oxide bonds, vibrations of the longitudinal optical (LO) phonons will build up an electric field along the direction of vibration. This field will interact with electrons and holes (known as the polaron effect), resulting in a change in the effective masses. The polaron mass m_p can be estimated from the energy of the LO phonon, $\hbar\omega_{LO}$, and the dielectric constants $\varepsilon(0)$ and $\varepsilon(\infty)$, assuming non-degenerate bands, harmonic oscillation of the ions, interactions only with long wavelength phonons (with constant frequency ω_{LO}), and the effective mass approximation: [15,16]

$$m_p = m \cdot (1 - \alpha/6)^{-1} \tag{2a}$$

$$\alpha = \frac{e^2 \sqrt{2m\omega_{LO}/\hbar}}{8\pi\varepsilon(0)\hbar\omega_{LO}} \left(\frac{1}{\varepsilon(\infty)} - \frac{1}{\varepsilon(0)} \right) \tag{2b}$$

where α is the Fröhlich constant. For the static (i.e., $\omega \approx 0$) and the high-frequency (i.e., $0 << \omega << E_g/\hbar$) dielectric constants we use the calculated values as given below. The optical phonon frequency is taken to be the experimental neutron-scattering value $\hbar\omega_{LO}$ = 46 meV by Traylor *et al.* [17], supported by the calculated phonon frequencies by Lee *et al* [18].

The effective hole masses depends strongly on the spin-orbit interaction. It has been demonstrated that the effective hole masses can be affected by as much as 15 times [19], and in cubic AlN the hole mass is negative unless spin-orbit interaction is taken into

account [20]. It is primarily the hole masses that are affected by the spin-orbit interaction, since the main effects are due to lifting band degeneracies [19,20]. In Table I we present the calculated effective bare electron and hole masses, as well as the corresponding polar masses, using the fully relativistic Hamiltonian (i.e., including the spin-orbit interaction). The anisotropy of the electronic band curvature can be represented by the ratio between transverse and longitudinal masses, and for the lowest conduction band $m_\perp/m_\parallel = 2.35$. The large polaron effect is due to low phonon frequency, and the large difference between $\varepsilon(0)$ and $\varepsilon(\infty)$ [see Eq. (2)].

mass (m_0)	2nd CB, m_{c2}		1st CB, m_{c1}		1st VB, m_{v1}		2nd VB, m_{v2}		3rd VB m_{v3}	
	m	m_p	m	m_p	m	m_p	m	m_p	m	m_p
$m_\perp$	0.88	1.59	1.41	2.52	1.74	4.53	0.54	0.82	0.54	0.82
$m_\parallel$	1.14	1.79	0.60	0.97	2.98	6.38	0.94	1.33	0.94	1.33

Table I. Transverse ($\perp$) and longitudinal ($\parallel$) effective electron m_c and hole m_v masses (in units of m_0) and the corresponding polaron masses m_p of the two lowest conduction bands (CBs) where c_1 is the lowest CB, and the three uppermost valence bands (VBs).

The dielectric function $\varepsilon(\omega) = \varepsilon_1(\omega) + i\varepsilon_2(\omega)$ of the semiconductors describe the response of the material due to a change in the charge distribution. The dielectric function is thus an important property for describing the screening of the semiconductor near dopants, defects, and other structural perturbations of the crystal. Within the linear response theory the dielectric function in the long wave length limit ($|\mathbf{k}'-\mathbf{k}| = 0$) is calculated directly from the electronic structure via the joint density-of-states and the optical momentum matrix elements. The imaginary part of the dielectric function is obtained as

$$\varepsilon_2^{xy}(\omega) = \frac{4\pi^2 e^2}{\Omega m_0^2 \omega^2} \sum_{\mathbf{k},j,j',\sigma} \langle \mathbf{k}, j, \sigma | \hat{p}_x | \mathbf{k}, j', \sigma \rangle \langle \mathbf{k}, j', \sigma | \hat{p}_y | \mathbf{k}, j, \sigma \rangle \times f_{\mathbf{k}j} \cdot (1 - f_{\mathbf{k}j'}) \cdot \delta(E_{j'}(\mathbf{k}) - E_j(\mathbf{k}) - \hbar\omega) \tag{3}$$

Here, e is the electron charge, m_0 its mass, Ω is the crystal volume and f_{kn} is the Fermi distribution. Moreover, $|\mathbf{k}j\sigma\rangle$ is the crystal wave function corresponding to the j:th eigenvalue $E_j(\mathbf{k})$ with crystal momentum $\mathbf{k}$ and spin σ. The $\mathbf{k}$-space summation is calculated using the modified tetrahedron interpolation with a $\mathbf{k}$-mesh containing about uniformly distributed 432 $\mathbf{k}$-points in the irreducible part of the Brillouin zone. The delta Dirac function in Eq. (3) indicates that a correct description of the fundamental band-gap energy is important to obtain dielectric function. The real part of the dielectric function is obtained from the Kramers-Kronig transformation relation

$$\varepsilon_1(\omega) = 1 + \frac{1}{2\pi} \int d\omega' \varepsilon_2(\omega') \left(\frac{1}{\omega' - \omega} + \frac{1}{\omega' + \omega} \right) \tag{4}$$

The electronic structure calculations do not include electron-phonon interactions. However, in polar semiconductors the optical phonons play an important role for the low-frequency dielectric function. The static $\varepsilon_1(0)$ dielectric constant can in polar materials be determined only by taking into account the electron-phonon interactions. The screening from the

electron-optical phonon (*ep*) interaction can approximately be taken into account through a delta function in $\varepsilon_2(\omega)$ at the transverse phonon frequency ω_{TO} assuming constant optical phonon frequency distribution [21]

$$\varepsilon_2^{ep}(\omega) = \delta(\omega - \omega_{TO})\pi\varepsilon_1(\infty)\frac{(\omega_{LO}^2 - \omega_{TO}^2)}{2\omega_{TO}}. \tag{5}$$

We employ the experimental values [17,18] of the two phonon frequencies ω_{LO} and ω_{TO}. The calculated imaginary part of the dielectric function [Fig. 2(a)] show onset to absorption at about 3.2-3.5 eV, associated with the direct transitions at the Γ-point, corresponding to the fundamental band gap of 3.0 eV. The peak around 5 eV is associated with transition along the (001) direction. The Delta Dirac peak at $\hbar\omega_{TO}$ = 23 meV [cf. Eq. (3)] is not visible. The real part of the dielectric function [Fig. 2(b)] show the anisotropy of the dielectric function. At low energies (i.e., at and below the optical phonon frequencies) the effects due to the electron-phonon coupling [i.e., $\varepsilon_2^{ep}(\omega)$] are obvious [see inset in Fig. 2(b)]. The calculated static $\varepsilon_\perp(0)$ = 144 and $\varepsilon_\parallel(0)$ = 171 as well as the high-frequency $\varepsilon_\perp(\infty)$ = 6.4 and $\varepsilon_\parallel(\infty)$ = 7.4 dielectric constants are in good agreement with the experimental results of $\varepsilon_\perp(0)$ = 111, $\varepsilon_\parallel(0)$ = 257 [22], $\varepsilon_\perp(\infty)$ = 6.8 and $\varepsilon_\parallel(\infty)$ = 8.4 [17]. Our calculated dielectric tensor a somewhat less anisotropic that the experimental findings. The calculated $\varepsilon(\infty)$ is obtained as the zero-frequency dielectric function when the electron-phonon coupling is excluded, and one should therefore expect that the theoretical $\varepsilon(\infty)$ is somewhat lower than the experimental value [cf. Fig. 2(b)] obtained from the full spectrum at $0 << \hbar\omega << E_g$. Furthermore, the calculated $\varepsilon(0)$ depends for TiO_2 strongly on variations in the electronic dispersion and phonon frequencies, which is in accordance with the strong temperature dependence of the measured $\varepsilon(0)$ [22].

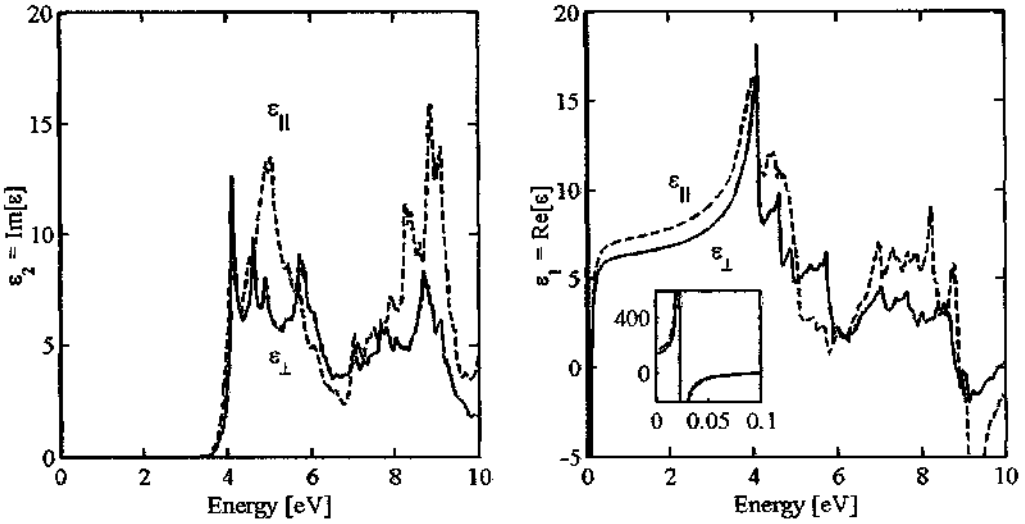

Figure 2. Transverse (⊥) and longitudinal (||) components of the (a) imaginary ε_2 and the (b) real ε_1 parts of the dielectric function $\varepsilon(\omega) = \varepsilon_1(\omega) + i\varepsilon_2(\omega)$ of rutile TiO_2.

SUMMARY

As demonstrated in this study, the LDA+U^{SIC} potential describes accurately the electronic band-edge structure of rutile TiO_2. The calculated fundamental band-gap energy E_g(LDA+U^{SIC}) = 2.97eV is similar to the previous room temperature measured value of 3.0 eV [6,14] . The advantage of the present LDA+U^{SIC} method is that the computational time is of the same order as the ordinary LDA calculations. The calculted effective electron and holes masses show strong anisotropic electronic band edges. We present both the bare effective masses and the corresponding polaron masses, where values of effective hole masses depends strongly on the spin-orbit interaction [19,20]. The optical properties of rutile TiO_2 are calculated in terms of the dielectric function. By taken into account the absorption of the optical phonons we calculate both the static $\varepsilon(0) = [2\varepsilon_{\perp}(0) + \varepsilon_{\parallel}(0)]/3 = 153$ as well as the high-frequency $\varepsilon(\infty) = [2\varepsilon_{\perp}(\infty) + \varepsilon_{\parallel}(\infty)]/3 = 6.7$ dielectric constants. These results are in good agreement with the experimental findings of $\varepsilon(0) = 159.6$ [22] and $\varepsilon(\infty) = 7.3$ [17] respectively.

ACKNOWLEDGMENTS

This work was financially supported in part by the Swedish Research Council (VR), the Swedish Foundation for International Cooperation in Research and Higher Education (STINT), Brazilian National Research Council (CNPq), CNPq/NanoSemiMat under grant no. 550.015/01-9, CNPq/REMAN under grant no. 400601/2004-4 and Fundacao de Amparo a Pesquisa do Estado da Bahia (FAPESB).

REFERENCES:

[1] K. Kim, C. G. Hwang and J. G. Lee, IEEE Trans. Electron Devices **45**, 598 (1998).
[2] S. A. Campbell, *et al.*, IEEE Trans. Electron Devices **44**, 104 (1997).
[3] S. Matsuda and A. Kato, Appl. Catal. **8**, 149 (1983).
[4] C. Persson and S. Mirbt (unpublished).
[5] P. Blaha, K. Schwarz, G.K.H. Madsen, D. Kvasnicka. and J. Luitz, WIEN2k, An APW + local orbitals program for calculating crystal properties (K. Schwarz, Techn. U. Wien, Austria), 2001.
[6] A. Ferreira da Silva, I. Pepe, C. Persson, J. Souza de Almeida, C. Moysés Araújo, R. Ahuja, B. Johansson, C.Y. An, and J.H. Guo, Phys. Scripta **T109** (2004) 180-184
[7] M. T. Czyzyk and G. A. Sawatzky, Phys. Rev. B **49**, 14211 (1994); V. I. Anisimov, I. V. Solovyev, M. A. Korotin, M. T. Czyzyk, and G. A. Sawatzky, Phys. Rev. B **48**, 16929 (1993); A. I. Liechtenstein, V. I. Anisimov, J. Zaanen, Phys. Rev. B **52**, R5467 (1995); P. Novák, F. Boucher, P. Gressier, P. Blaha, and K. Schwarz, Phys. Rev. B **63**, 235114 (2001).
[8] J. P. Perdew and M. Levy, Phys. Rev. Lett. **51**, 1884 (1983); L. J. Sham and M. Schlüter, Phys. Rev. Lett. **51**, 1888 (1983).

[9] M. Städele, J. A. Majewski, P. Vogl, and A. Görling, Phys. Rev. Lett. **79**, 2089 (1997); M. Städele, M. Moukara, J. A. Majewski, P. Vogl, and A. Görling, Phys. Rev. B **59**, 10031 (1999).
[10] N. E. Christensen, Phys. Rev. B **30**, 5753 (1984); C. Persson, R. Ahuja, and B. Johansson, Phys. Rev. B **64**, 033201 (2001).
[11] *Physics of Group IV Elements and III–V Compounds*, edited by O. Madelung *et al.*, Landolt- Börnstein, New Series, Group III, Vol. 17a (Springer, Berlin, 1982).
[12] C. Persson and A. Zunger, Phys. Rev. B **68**, 073205 (2003).
[13] C. L. Dong, C. Persson, L. Vayssieres, A. Augustsson, T. Schmitt, M. Mattesini, R. Ahuja, C. L. Chang, and J.-H. Guo, to appear in Phys. Rev. B.
[14] A. Ferreira da Silva, N. Souza Dantas, E. F. da Silva, Jr, I. Pepe, M. O. Torres, C. Persson, T. Lindgren, J. Souza de Almeida, and R. Ahuja, Phys. Stat. Sol. (c) (to appear 2004).
[15] C. Persson, U. Lindefelt, and B. E. Sernelius, Phys. Rev. B 60, 16479 (1999).
[16] *Polarons in Ionic Crystals and Polar Semiconductors*, edited by J. T. Devreese (North-Holland, Amsterdam, 1972).
[17] J. G. Traylor, H. G. Smith, R. M. Nicklow, and M. K. Wilkinson, Phys. Rev. B **3**, 3457 (1971).
[18] C. Lee, P. Ghosez, and X. Gonze, Phys. Rev. B **50**, 13379 (1994).
[19] C. Persson and U. Lindefelt, J. Appl. Phys. **82**, 5496 (1997).
[20] C. Persson, A. Ferreira da Silva, R. Ahuja, and B. Johansson, J. Cryst Growth **231**, 397 (2001).
[21] C. Persson, R. Ahuja, A. Ferreira da Silva, and B. Johansson, J. Phys.: Condens. Matter, **13**, 8945 (2001); *ibid* J. Cryst. Growth **231**, 407 (2001).
[22] R. A. Parker, Phys. Rev. **124**, 1719 (1961).
[23] T. Lindgren , J. M. Mwabora, E. Avendaño, J. Jonsson, A Hoel, C.-G. Granqvist and S. –E. Lindquist, J. Phys. Chem. B**107**, 5709 (2003).
[24] S. A Tomas, S. Stolik, R. Palomino, R. Lozada, C. Persson, R. Ahuja, I. Pepe, and A Ferreira da Silva, J. de Physique IV (to appear).